AIAA JOURNAL
Vol. 43, No. 9, September 2005

Stability Analysis of a Delaminated Beam Subjected to Follower Compression

Q. Wang,* F. Moslehy,† and D. W. Nicholson†
University of Central Florida, Orlando, Florida 32816-2450

A stability analysis of a delaminated beam subjected to a follower compressive load is presented. The beam is fixed at its left end and restrained by a translational spring at its right end as this specific configuration of beam subjected to follower force has garnered great interest among the structural community. The vibration analysis on this delaminated beam is conducted to identify the critical compression load for flutter or buckling instability for the beam. In addition, the critical spring stiffness is derived to determine the distinct type of instability of the beam under the follower compression. Furthermore, the effect of the location of the delamination both in the thickness and the longitudinal direction and the length of the delamination on the critical compressive load for buckling or flutter instability of the beam is completely studied through a mechanics analysis. It is hoped that this research would provide a benchmark on the stability analysis of delaminated structures in engineering applications, especially for structures subjected to follower compressive load.

Introduction

ANALYSIS of flutter and buckling of beams has been an interesting subject in the applied mechanics community. The mathematical solutions for the buckling load of beams subjected to nonfollower compression with different boundary conditions were given in the monograph of Timoshenko and Gere.[1] Flutter analysis of a cantilever beam subjected to follower compression was also briefly introduced in the monograph. Beam buckling is an instability phenomenon where the change of equilibrium state from one configuration to another occurs at a critical compression value. On the other hand, flutter is an instability phenomenon in which the vibration amplitude caused by initial disturbance grows without limit when the follower compression exceeds a critical value.

Buckling is usually caused by both nonfollower compression and follower compression subjected to the beams. However, flutter can only occur in beams subjected to follower compression. A nonfollower force is usually referred as an axial force with its direction remaining constant during the deformation of the structure. A follower force, on the other hand, is different from the nonfollower force just mentioned in the sense that the direction of this type of force remains tangent to the deflection curve at the top of the column.[1]

Buckling and flutter analysis of healthy or undamaged beam structures under follower force has been addressed by many research efforts. Bolotin[2] studied a classical problem about the stability of a beam fully fixed at one end and subjected at the other end to a tangential compressive follower force. Feodosév[3] and Pfluger[4] showed that there are no buckling solutions for this problem and concluded that the beam with follower force is stable all of the time. This erroneous conclusion was debated by Beck,[5] who first solved this flutter instability problem through dynamic analysis. Since then, the study of flutter instability has attracted substantial research interest. Carr and Malhardeen[6] and Leipholz[7] proved that Beck's column is stable when the follower force is less than the critical value obtained by Beck. Deineko and Leonov[8] studied the combined effect of nonfollower and follower compressions applied to a cantilever beam. The influence of an elastic support on the vibration and stability of a nonconservative load was studied by Sundararajan.[9] In his paper, the transition value of the translational spring at the free end of a cantilever beam was derived, and the coexistence of flutter and buckling in a system was first observed. Kounadis[10] presented an analysis of the existence of divergence instability regions for a general beam structure. Actually, buckling and flutter analysis can be categorized as a linearized approach in dealing with instability analysis of undamped structures. More complex instability studies on either undamped or damped structures under dynamic loading have been conducted as well. Some fruitful results have been obtained so far by Kounadis,[11,12] Bolotin et al.,[13] Ryu and Sugiyama,[14] Langthjem and Sugiyama,[15] and Andersen and Thompsen.[16] Wang[17] conducted a complex flutter and buckling analysis of a beam structure subjected to static follower force. The flutter and buckling analysis of a beam subjected to a follower force and constrained by a pair of transverse and rotational springs at one end and fixed at the other end was studied theoretically.[18] The effects of the transverse and rotational spring stiffness were studied to obtain the transition condition differentiating two distinct types of instability that coexisted in the beam. In the theoretical models of all of the preceding works, the left boundary of the beam subjected to follower force was all modeled with either fixed end or end with restriction of displacement in the flexural direction to maintain the equilibrium state of the beam. Such a standard configuration has provided a great and powerful model in studying most of flutter-related stability problems in beam structures. Flutter instability of beams with other boundary conditions, such as free-free edges, was investigated via finite element analysis.[19]

More research on the buckling and/or flutter load of damaged beams subjected to follower compression is critical for a better design and health monitoring of such beams. The stability of a cracked column was studied experimentally and analytically[20–22] by considering the local flexibility at the crack as a spring. However, few reports have been found on the analyses of the buckling and/or flutter load of cracked beams subjected to follower compression. Wang[23] proposed a comprehensive stability analysis of a cracked beam subjected to a follower compression.

Composite materials have received increased attention in recent years, especially for aeronautical and marine applications. Delamination in composites has been a topic of concern in such applications. This has been extensively reviewed by Wilkins et al.[24] The accompanying problem of buckling of delaminated composite laminates has been widely studied by many researchers.[25–27] Troshin[28] addressed primarily the question of delamination buckling in dealing with a pressure-loaded laminar cylindrical shell. Peck

Received 17 November 2004; revision received 17 February 2005; accepted for publication 25 February 2005.

*Associate Professor, Mechanical, Materials and Aerospace Engineering Department, 4000 Central Florida Boulevard; qzwang@mail.ucf.edu.

†Professor, Mechanical, Materials and Aerospace Engineering Department, 4000 Central Florida Boulevard.

and Springer[29] investigated the behavior of elliptical sublaminates initiated by delamination in composite plates that are subjected to in-plane compression, shear, and thermal loads. Lee et al.[30] considered both vibration and buckling of delaminated structures. The effect of the delamination opening was taken into account by using the relative position between the sublaminates as proposed by Luo and Hanagud[31] and Lestari and Hanagud.[32] However, it is noted that few studies on the stability analysis of the delaminated beams are focused on the stability analysis of structures subjected to follower compression.

The research in this paper will provide a stability analysis of a delaminated beam subjected to a follower compressive load. Because, as just indicated, the beam with one end fixed is a standard configuration for the analysis of most of flutter related analysis of beams via theoretical models, the beam under investigation in the current research is fixed at the left end and restrained by a translational spring at its right end. The flutter or buckling load of the delaminated beam will be obtained through dynamic analysis of the beam. The transition spring stiffness differentiating flutter and buckling of the delaminated beam is first derived similar to the work for cracked beam.[33] The effect of the size of the delamination and the location of the delamination both in longitudinal and thickness direction of the beam will be provided via a detailed mechanics analysis. The research method is strictly based on an undamped linearized approach. The coexisting instability phenomena of the delaminated beam structure are important in the field of structural stability and dynamics, as the understanding of the instability nature of a delaminated structure will be helpful for its stability design.

Mechanics Model for the Stability Analysis of the Delaminated Beam

The stability analysis of a beam with a horizontally aligned delamination shown in Fig. 1 subjected to a follower axial force P is to be studied here. The material and geometric parameters of the delaminated beam are denoted as E for the Young's modulus of the host beam, H for the thickness of the beam, h for the distance of the delamination from the top of the host beam, a for the length of the delamination, L_1 and L_2 for the respective distances of the left tip of the delamination to the left end of the beam and the right tip of the delamination to the right end of the beam, and k for the stiffness of the spring attached at the right end of the beam. A comprehensive mechanics analysis will be conducted here to investigate the effect of the delamination on the beam structure. The delamination part will be studied via Euler–Bernoulli beam theory by considering two layers of beam elements connected at the two ends. The interface of the two layers is considered as connection of two free surfaces. Because the midplanes of the two layers are off the midplane of the delaminated beam, axial elongation and compression on the two layers will thus be induced as a result of the bending of the beam. It is assumed the incremental tensile force Δp_1 and compressive force Δp_2 are induced on the top and bottom layers of the delamination. The bending motion is only considered here to derive the induced Δp_1 and Δp_2 for stability analysis because the lateral and axial motions in a beam structure are decoupled. Thus, it can be understood that the following bending analysis of the delaminated beam is conducted with respect to the deformed beam in its longitudinal direction caused by the compressive loading. Because of the

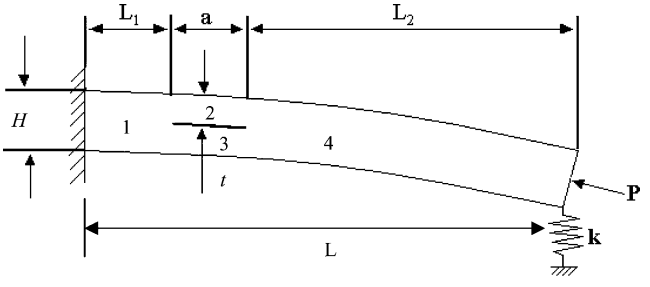

Fig. 1 Layout of delaminated beam subjected to follower force.

continuity of the deflection at the left tip of the delamination based on beam theory, we have

$$u_{1L} - \tfrac{1}{2}w'_L|_{x=x_l}(H-t) = u_{0L} \tag{1a}$$

$$u_{2L} - \left[-(t/2)w'_L|_{x=x_l}\right] = u_{0L} \tag{1b}$$

where w_L is the flexural deflection of the beam element at the left side of the delamination, x_l is the coordinate of the left tip of the delamination, prime indicates the derivative with respect of x, u_{1L} and u_{2L} indicate the horizontal displacement of the midplane of the upper and lower layers of the delamination at the left tip, and u_{0L} is the horizontal displacement of the midplane of the delaminated beam at the left tip of the beam. Similarly, at the right tip of the delamination we have

$$u_{1R} - \tfrac{1}{2}w'_R|_{x=x_r}(H-t) = u_{0R} \tag{2a}$$

$$u_{2R} - \left[-(t/2)w'_R|_{x=x_r}\right] = u_{0R} \tag{2b}$$

where w_R is the deflection of the beam section on the right side of the delamination, x_r is the coordinate of the right tip of the delamination, u_{1R} and u_{2R} indicate the midplane horizontal displacements of the upper and lower layers of the delamination at the right tip, and u_{0R} is the horizontal displacement of the midplane of the delaminated beam at the right tip of the beam.

The elongation and the compression of the midplane of the two layers can be expressed, respectively, as

$$u_{1R} - u_{1L} = \Delta p_1 a/EtT \tag{3a}$$

$$u_{2R} - u_{2L} = -\Delta p_2 a/E(H-t)T \tag{3b}$$

where T is the width of the beam.

The characteristic of the nondeformable midplane of the delaminated beam implies $u_{0R} - u_{0L} = 0$. Comparison of Eqs. (3a) and (3b) and Eqs. (1a) and (1b) and (2a) and (2b) leads to

$$\Delta p_1 a/EtT + \Delta p_2 a/ET(H-t) = -(H/2)\left(w'_L|_{x=x_l} - w'_R|_{x=x_r}\right) \tag{4a}$$

$$\Delta p_1 = \Delta p_2 \tag{4b}$$

and finally we have

$$\Delta p_1 = \Delta p_2 = -(ETH\beta/2a)\left(w'_L|_{x=x_l} - w'_R|_{x=x_r}\right) \tag{5}$$

where

$$\beta = [1/t + 1/(H-t)]^{-1}$$

The preceding mechanics analysis shows that at the tip of the delamination tensile and compressive forces are induced at the upper and lower part of the tip as a result of the bending of the beam as shown in Fig. 2a. The induced tensile and compressive forces will lead to the discontinuity of the shear force at the tip of the delamination, which will definitely result in the shear-force singularity. Therefore, the effect of the delamination on the stability analysis of the delaminated beam has to be examined because of the existence of the shear-force singularity by the delamination so that an appropriate stability design of the delaminated beam becomes possible.

The stability analysis of the beam structure will be obtained from a free-vibration analysis conducted hereinafter. The beam is partitioned into four sections shown in Fig. 1. The governing equation of the delaminated beam for section 1 is

$$EI\frac{\partial^4 w_1(x_1,t)}{\partial x_1^4} + P\frac{\partial^2 w_1(x_1,t)}{\partial x_1^2} + \rho A\frac{\partial^2 w_1(x_1,t)}{\partial t^2} = 0$$

$$0 \le x_1 \le L_1 \tag{6}$$

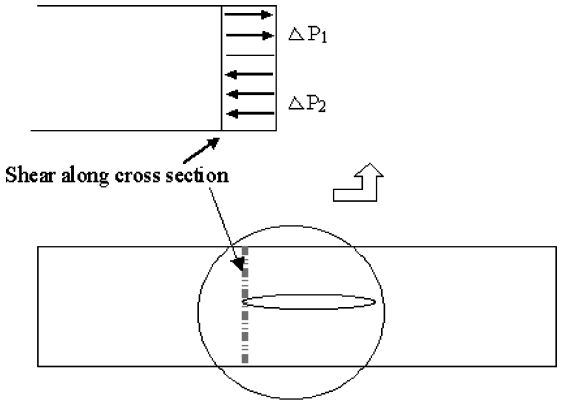

Fig. 2a Fracture mechanism at the tip of the delamination.

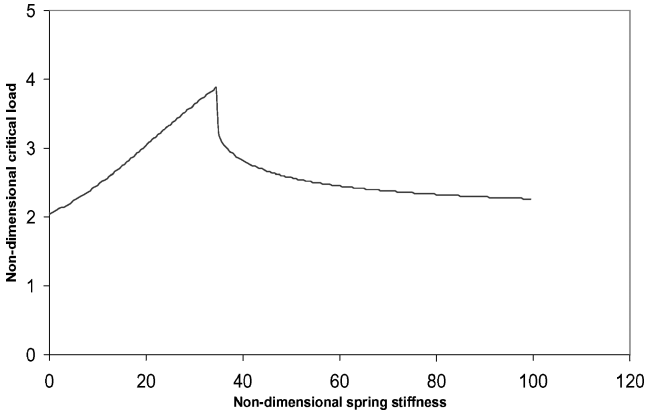

Fig. 2b Critical compressive load vs the nondimensional spring stiffness.

where the area moment of inertia of the cross section is $I = H^3/12$ assuming the width of the delamination of the beam is unit and A is the area of the cross section.

By using the method of variable separation given by $w_1(x_1, t) = W_1(x_1)e^{i\omega t}$, we can find the analytical solution for the mode shape function $W_1(x_1)$ directly:

$$W_1(x_1) = A_1 \cos k_1 x_1 + A_2 \sin k_1 x_1 + A_3 \cosh k_2 x_1 + A_4 \sinh k_2 x_1 \tag{7}$$

where

$$k_1 = \left(\lambda/2 + \sqrt{\lambda^2/4 + \mu^2}\right)^{\frac{1}{2}}, \qquad k_2 = \left(-\lambda/2 + \sqrt{\lambda^2/4 + \mu^2}\right)^{\frac{1}{2}}$$

and $\lambda = P/EI$ and $\mu^2 = \rho A\omega^2/EI$; $A_i (i = 1, \ldots, 4)$ are four constants.

Applying the left-end fixed boundary conditions, $W_1(0) = 0$, $\mathrm{d}W_1(x_1)/\mathrm{d}x_1|_{x_1=0} = 0$, to the general solution, Eq. (7), yields

$$W_1(x_1) = A_3(\cosh k_2 x_1 - \cos k_1 x_1) + A_4[\sinh k_2 x_1 - (k_2/k_1)\sin k_1 x_1] \tag{8}$$

Similarly the expression for the mode shape function $W_4(x_4)$ on section 4 can be written as follows, by considering the boundary conditions of the beam on its right end:

$$\left.\frac{\mathrm{d}^2 W_4(x_4)}{\mathrm{d}x_4^2}\right|_{x_4=L} = 0, \qquad \left.\frac{\mathrm{d}^3 W_4(x_4)}{\mathrm{d}x_4^3}\right|_{x_4=L} - \frac{\bar{k}}{L^3} W_4(L) = 0 \tag{9a}$$

$$W_4(x_4) = B_3(\cosh k_2 x_4 + N_1 \cos k_1 x_4 + N_3 \sin k_1 x_4) + B_4(\sinh k_2 x_4 + N_4 \sin k_1 x_4 + N_2 \cos k_1 x_4) \qquad 0 \le x_4 \le L_2 \tag{9b}$$

where the nondimensional spring stiffness is given by $\bar{k} = kL^3/EI$ and $N_i (i = 1, 2, 3, 4)$ are given in the Appendix.

A general model for the effect of delamination is provided in Refs. 31 and 32. The behavior of the effects between the delaminated sublaminates was described by a nonlinear spring model simplified into a piecewise linear model. The linear model for the delamination part based on their work is expressed as follows for the upper and lower layers:

$$EI_1 \frac{\partial^4 w_2(x_2, t)}{\partial x_2^4} + P_1 \frac{\partial^2 w_2(x_2, t)}{\partial x_2^2} + \rho A_1 \frac{\partial^2 w_2(x_2, t)}{\partial t^2} = k_1[w_3(x_2, t) - w_2(x_2, t)] \qquad 0 \le x_2 \le a \tag{10}$$

$$EI_2 \frac{\partial^4 w_3(x_2, t)}{\partial x_2^4} + P_2 \frac{\partial^2 w_3(x_2, t)}{\partial x_2^2} + \rho A_2 \frac{\partial^2 w_3(x_2, t)}{\partial t^2} = -k_1[w_3(x_2, t) - w_2(x_2, t)] \qquad 0 \le x_2 \le a \tag{11}$$

where $I_1 = I\bar{t}^3$, $I_2 = I(1-\bar{t})^3$, $P_1 = P\bar{t}$, $P_2 = P(1-\bar{t})$, $A_1 = A\bar{t}$, $A_2 = A(1-\bar{t})$, $\bar{t} = h/H$, and k_1 is the parameter characterizing the nature of closing and opening of the delamination. The case $k_1 = 0$ stands for the model of an unconstrained delaminated beam. Such a simple model has widely been adopted in studying stability analysis of delaminated beam.[25,26] Therefore, this unstrained delaminated beam model is employed to study the flutter analysis of the delaminated. More complicated delamination conditions are beyond the scope of the manuscript and will be investigated in future work.

The general solutions for the mode shapes $W_2(x_2)$ and $W_3(x_2)$ in Eqs. (10) and (11) at $k_1 = 0$ are directly shown separately:

$$W_2(x_2) = C_1 \cos k_{11} x_2 + C_2 \sin k_{11} x_2 + C_3 \cosh k_{21} x_2 + C_4 \sinh k_{21} x_2 \tag{12}$$

$$W_3(x_2) = D_1 \cos k_{12} x_2 + D_2 \sin k_{12} x_2 + D_3 \cosh k_{22} x_2 + D_4 \sinh k_{22} x_2 \tag{13}$$

where

$$k_{11} = \left(\lambda_1/2 + \sqrt{\lambda_1^2/4 + \mu_1^2}\right)^{\frac{1}{2}}$$

$$k_{21} = \left(-\lambda_1/2 + \sqrt{\lambda_1^2/4 + \mu_1^2}\right)^{\frac{1}{2}}$$

$$k_{12} = \left(\lambda_2/2 + \sqrt{\lambda_2^2/4 + \mu_2^2}\right)^{\frac{1}{2}}$$

$$k_{22} = \left(-\lambda_2/2 + \sqrt{\lambda_2^2/4 + \mu_2^2}\right)^{\frac{1}{2}}$$

$$\lambda_1 = P_1/EI_1 = \lambda/\bar{t}^2, \qquad \lambda_2 = P_2/EI_2 = \lambda/(1-\bar{t})^2$$

$$\mu_1^2 = \rho A_1\omega^2/EI_1 = \mu^2/\bar{t}^2, \qquad \mu_2^2 = \rho A_2\omega^2/EI_2 = \mu^2/(1-\bar{t})^2$$

To derive the resonant frequencies of the delaminated beam, the continuity conditions for the deflection and rotation at both the interface of sections 1 and 2 and the interface of sections 1 and 3 are provided hereinafter:

$$W_1(L_1) = W_2(0) \tag{14a}$$

$$W_1(L_1) = W_3(0) \tag{14b}$$

$$\left.\frac{\mathrm{d}W_1(x_1)}{\mathrm{d}x_1}\right|_{x_1=L_1} = \left.\frac{\mathrm{d}W_2(x_2)}{\mathrm{d}x_2}\right|_{x_2=0} \tag{14c}$$

$$\left.\frac{\mathrm{d}W_1(x_1)}{\mathrm{d}x_1}\right|_{x_1=L_1} = \left.\frac{\mathrm{d}W_3(x_2)}{\mathrm{d}x_2}\right|_{x_2=0} \tag{14d}$$

Because incremental tensile and compressive forces are induced at the upper and lower layers of the delamination, additional moment

caused by the induced tensile and compressive forces can thus be expressed as

$$\Delta M = \Delta p_1[(H-h)/2] + \Delta p_2(h/2) = \Delta p_1 H/2 \tag{15}$$

Therefore, the continuity of the shear force and the discontinuity of the moment both at the interface of sections 1 and 2 and the interface of sections 1 and 3 are expressed as follows by considering the expression of Δp_1 in Eq. (5):

$$EI\frac{\mathrm{d}^2W_1(x_1)}{\mathrm{d}x_1^2}\bigg|_{x_1=L_1} = EI_1\frac{\mathrm{d}^2W_2(x_2)}{\mathrm{d}x_2^2}\bigg|_{x_2=0} + EI_2\frac{\mathrm{d}^2W_3(x_2)}{\mathrm{d}x_2^2}\bigg|_{x_2=0} + \frac{\Delta p_1 H}{2}$$

that is,

$$\frac{\mathrm{d}^2W_1(x_1)}{\mathrm{d}x_1^2}\bigg|_{x_1=L_1} = \bar{t}^3\frac{\mathrm{d}^2W_2(x_2)}{\mathrm{d}x_2^2}\bigg|_{x_2=0} + (1-\bar{t})^3\frac{\mathrm{d}^2W_3(x_2)}{\mathrm{d}x_2^2}\bigg|_{x_2=0} - \frac{\beta[W_2(0)-W_2(a)]}{3a} \tag{16a}$$

$$EI\frac{\mathrm{d}^3W_1(x_1)}{\mathrm{d}x_1^3}\bigg|_{x_1=L_1} = EI_1\frac{\mathrm{d}^3W_2(x_2)}{\mathrm{d}x_2^3}\bigg|_{x_2=0} + EI_2\frac{\mathrm{d}^3W_3(x_2)}{\mathrm{d}x_2^3}\bigg|_{x_2=0}$$

that is,

$$\frac{\mathrm{d}^3W_1(x_1)}{\mathrm{d}x_1^3}\bigg|_{x_1=L_1} = \bar{t}^3\frac{\mathrm{d}^3W_2(x_2)}{\mathrm{d}x_2^3}\bigg|_{x_2=0} + (1-\bar{t}^3)\frac{\mathrm{d}^3W_3(x_2)}{\mathrm{d}x_2^3}\bigg|_{x_2=0} \tag{16b}$$

Similarly, the continuity conditions for deflection and rotation at the interface of sections 2 and 4 and the interface of sections 3 and 4 are shown as

$$W_2(a) = W_4(0) \tag{17a}$$

$$W_3(a) = W_4(0) \tag{17b}$$

$$\frac{\mathrm{d}W_2(x_2)}{\mathrm{d}x_2}\bigg|_{x_2=a} = \frac{\mathrm{d}W_4(x_4)}{\mathrm{d}x_4}\bigg|_{x_4=0} \tag{17c}$$

$$\frac{\mathrm{d}W_3(x_2)}{\mathrm{d}x_2}\bigg|_{x_2=a} = \frac{\mathrm{d}W_4(x_4)}{\mathrm{d}x_4}\bigg|_{x_4=0} \tag{17d}$$

and shear-force continuity and moment discontinuity at the interface are therefore expressed as follows:

$$\bar{t}^3\frac{\mathrm{d}^2W_2(x_2)}{\mathrm{d}x_2^2}\bigg|_{x_2=a} + (1-\bar{t})^3\frac{\mathrm{d}^2W_3(x_2)}{\mathrm{d}x_2^2}\bigg|_{x_2=a} - \frac{\beta[W_2(0)-W_2(a)]}{3a} = \frac{\mathrm{d}^2W_4(x_4)}{\mathrm{d}x_4^2}\bigg|_{x_4=0} \tag{18a}$$

$$\bar{t}^3\frac{\mathrm{d}^3W_2(x_2)}{\mathrm{d}x_2^3}\bigg|_{x_2=a} + (1-\bar{t})^3\frac{\mathrm{d}^3W_3(x_2)}{\mathrm{d}x_2^3}\bigg|_{x_2=a} = \frac{\mathrm{d}^3W_4(x_4)}{\mathrm{d}x_4^3}\bigg|_{x_4=0} \tag{18b}$$

Substitution of the expressions for $W_1(x_1)$, $W_2(x_2)$, $W_3(x_2)$, and $W_4(x_4)$ from Eqs. (8), (9b), (12), and (13) into the continuity conditions in Eqs. (14a–14d), (16a–16d), (17a–17d), and (18a) and (18b) leads to the following homogeneous equation for the coefficients A_3, A_4, B_3, B_4, C_i, and $D_i (i = 1, 2, 3, 4)$:

$$[C]\begin{Bmatrix} C_1 \\ C_2 \\ C_3 \\ C_4 \\ D_1 \\ D_2 \\ D_3 \\ D_4 \\ A_3 \\ A_4 \\ B_3 \\ B_4 \end{Bmatrix} = \begin{Bmatrix} 0 \\ 0 \\ 0 \\ 0 \\ 0 \\ 0 \\ 0 \\ 0 \\ 0 \\ 0 \\ 0 \\ 0 \end{Bmatrix} \tag{19}$$

where $[C]$ is the coefficient matrix whose nonzero elements are listed in the Appendix.

The instability of the beam, either for buckling or flutter, will be derived from the condition for the nontrivial solution for A_3, A_4, B_3, B_4, C_i, and $D_i (i = 1, 2, 3, 4)$, from Eq. (19), which is

$$det[C] = 0 \tag{20}$$

The occurrence of the flutter or buckling load of the delaminated beam subjected to the follower force will be determined from the variation of the first two frequencies of the structure. For a given follower force P, the first two resonant frequencies ω_1 and ω_2 can be obtained from Eq. (20). There is, however, a definite value of the follower force P at which the values of ω_1 and ω_2 approach each other.[1] We define the definite value of the follower force as critical load for the flutter of the beam structure. On the other hand, we define the value of the follower force as the critical load for the buckling of the structure if the value of ω_1 reaches zero.

Numerical Results and Discussion

Numerical simulations are conducted for a stability analysis of the delaminated beam structure subjected to follower force in Fig. 1. The following nondimensional parameters will be employed in the simulations: follower force $\bar{P} = P/P_{\mathrm{cr}}$, where $P_{\mathrm{cr}} = \pi^2 EI/L^2$ is Euler buckling load; the location of delamination in longitudinal direction $\bar{L}_1 = L_1/L$; the location of delamination in flexural direction $\bar{t} = h/H$; and the length of the beam $\bar{a} = a/L$.

To the knowledge of the authors, no existed research results can be found for the flutter analysis of delaminated beam. Thus, the validation of the developed model is only investigated via the comparison of the buckling load of a clamped delaminated beam provided by Simitses et al.[26] The buckling load of a clamed delaminated beam from the current research can be derived by changing the first expression in Eq. (9a) by $W_4'(x_4) = 0$ and making $\bar{k}$ in the second expression of the equation to be a very large value, say, $\bar{k} = 1000$. The comparison is shown in Table 1 from which an excellent agreement can be observed.

Table 1 Comparison of the buckling load of a fixed-fixed delaminated beam with that of Simitses et al.[26] at $\bar{a} = 0.2$

	$\bar{L}_1 = 0.1$		$\bar{L}_1 = 0.2$		$\bar{L}_1 = 0.3$		$\bar{L}_1 = 0.4$	
$\bar{t}$	Present	Simitses	Present	Simitses	Present	Simitses	Present	Simitses
0.05	0.06249	0.06249	0.06249	0.06249	0.06249	0.06249	0.06249	0.06249
0.1	0.24999	0.24969	0.24999	0.24961	0.24999	0.24956	0.24999	0.24953
0.3	0.91499	0.91421	0.91999	0.91948	0.96249	0.96134	0.99249	0.99239
0.5	0.84124	0.84051	0.85625	0.85547	0.92875	0.92775	0.99624	0.99554

Table 2 Transition value of the spring stiffness for buckling and flutter at $\bar{t} = 0.5$

$\bar{L}_1$	$\bar{a} = 0.1$	$\bar{a} = 0.2$	$\bar{a} = 0.3$
0	35.1	39.2	23.4
0.1	35	30.9	13.7
0.2	33.9	25.5	11.5
0.4	34	32.2	34.7
0.6	35.4	37	24.4
0.7	34.4	28.2	13.3

Table 3 Transition value of the spring stiffness for buckling and flutter at $\bar{t} = 0.1$

$\bar{L}_1$	$\bar{a} = 0.1$	$\bar{a} = 0.2$	$\bar{a} = 0.3$
0	34.6	35.3	35.7
0.1	34.5	34.4	32.6
0.2	34.5	33.6	31.3
0.4	34.6	34.6	35.8
0.6	34.6	34.8	34.2
0.7	34.6	33.9	33.8

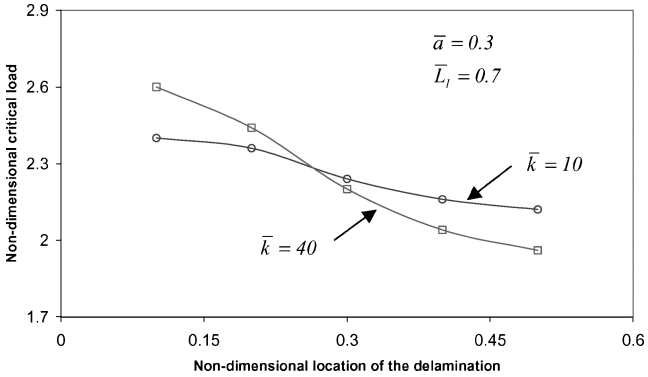

Fig. 3 Critical axial force vs the location of the delamination in the thickness direction.

The critical load for a healthy beam vs the stiffness of the spring at the right end of the beam is plotted in Fig. 2b (Ref. 23) from which an abrupt decrease of the load at $\bar{k} \approx 34.8$ is clearly observed from the figure. From the variation of the first two frequencies of the system, it can be concluded that $\bar{k} \approx 34.8$ is the critical stiffness of the spring, differentiating flutter and buckling instability of the beam. Only flutter can occur on the beam if the stiffness of the spring is less than the critical value; otherwise, only buckling instability will occur on the beam. This conclusion also coincides with the conclusion by Kounadis.[10] Thus, $\bar{k} \approx 34.8$ can be defined as the transition value of the spring stiffness for the flutter and buckling of healthy beam. The critical compressive load for flutter of a cantilever beam and for buckling of a propped cantilever beam can be read from Fig. 2b as $\bar{P} = 2.04$ and 2.05 if $\bar{k} = 0$ and ∞ are set, which are in agreement with those from the monograph of Timoshenko and Gere.[1]

The transition values of the spring stiffness for the delaminated beam vs the location of the delamination in the longitudinal direction at different lengths of the delamination at $\bar{t} = 0.5$ and 0.1 are listed in Tables 2 and 3, respectively. The first observation from the tables is that there are fewer differences in the transition values for shorter delamination for both $\bar{t} = 0.5$ and 0.1. The second observation is that if the delamination is placed near the surface of the beam, the transition values of the spring stiffness are all near the critical value for the healthy beam, that is, $\bar{k} \approx 34.8$, especially for shorter delamination. It can also be found that the variation of the value is similar for all the cases.

The effect of location of the delamination in its thickness direction $\bar{t}$ on the critical axial load $\bar{P}$ is illustrated in Fig. 3 at $\bar{k} = 10$ and 40 when $\bar{a} = 0.3$ and $\bar{L}_1 = 0.7$. The critical loads are $\bar{P} \approx 2.4$

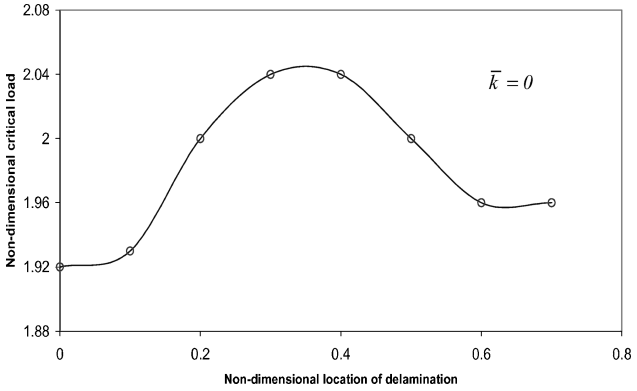

Fig. 4a Critical axial force vs the location of the delamination in the longitudinal direction: $\bar{k} = 0$.

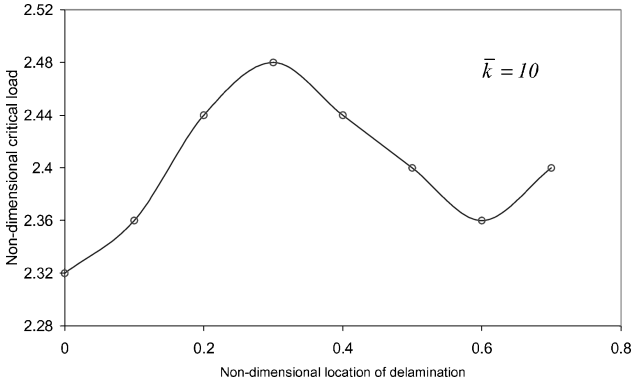

Fig. 4b Critical axial force vs the location of the delamination in the longitudinal direction: $\bar{k} = 10$.

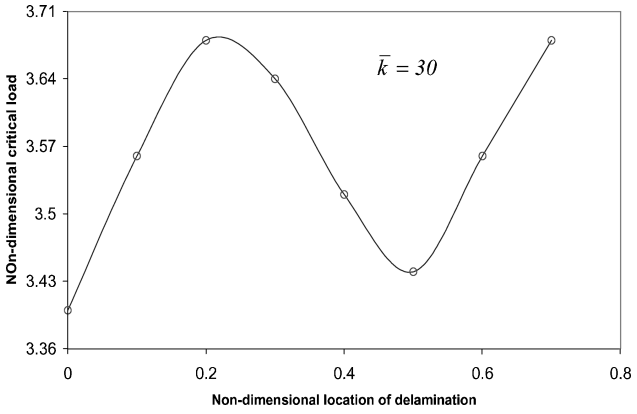

Fig. 4c Critical axial force vs the location of the delamination in the longitudinal direction: $\bar{k} = 30$.

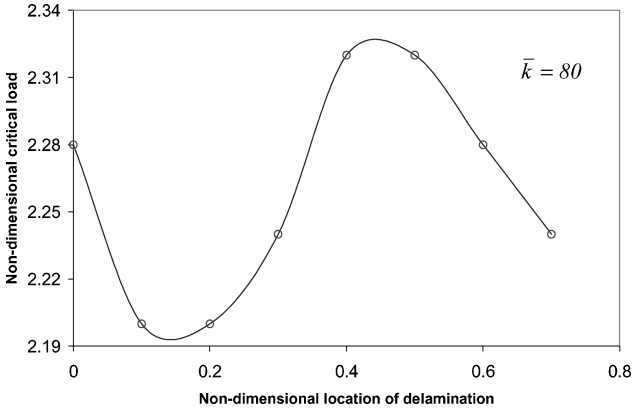

Fig. 4d Critical axial force vs the location of the delamination in the longitudinal direction: $\bar{k} = 80$.

Table 4 Critical load vs the location of the delamination in the longitudinal direction

	$\bar{a}=0.1$			$\bar{a}=0.2$		
$\bar{L}_1$	$\bar{k}=0$	$\bar{k}=30$	$\bar{k}=80$	$\bar{k}=0$	$\bar{k}=30$	$\bar{k}=80$
0	2.0216	3.6176	2.3142	2.0349	3.5644	2.3142
0.2	2.0216	3.6176	2.3142	2.0349	3.6176	2.2876
0.4	2.0216	3.6176	2.3142	2.0349	3.6043	2.3009
0.6	2.0216	3.6176	2.3142	2.0349	3.5777	2.3142
0.8	2.0216	3.6176	2.3142	2.0349	3.5245	2.2876

for $\bar{k}=10$ and $\bar{P}\approx 2.6$ for $\bar{k}=40$ at $\bar{t}=0.1$, which are almost the same as the solutions for the healthy beam. As indicated in Tables 2 and 3, these two values are flutter load and buckling load, respectively. Another observation is that the critical load decreases with increase in the location of the delamination in the flexural direction. In addition, the buckling load, that is, for the case at $\bar{k}=40$, decreases more obviously than the flutter load, that is, for the case at $\bar{k}=10$.

In all of the following simulations, the delamination is assumed to be located at $\bar{t}=0.1$ in the thickness direction. First, the variation of the critical load $\bar{P}$ vs the location of the delamination in the longitudinal direction for a cantilever beam, that is, $\bar{k}=0$, at $\bar{a}=0.3$ is shown in Fig. 4a. It is known that the flutter is the only instability form of the beam. It is noted from the figure that the delamination has the least effect on the stability of the beam when the delamination is around $\bar{L}_1=0.35$ because the critical load is around $\bar{P}=2.04$, which is the flutter load for a healthy beam, at this location. On the other hand, the delamination leads to a dramatic decrease of the critical load $\bar{P}$ when it is located around the left end and $\bar{L}_1=0.55$ as shown clearly in the simulation. Similar conclusions can also be derived from the variation of $\bar{P}$ in Figs. 4b and 4c at $\bar{k}=10$ and 30, respectively. The locations for the least effect and highest effect on the critical load move leftward with the increase of the spring stiffness. The location for the least effect of the delamintaion are $\bar{L}_1\approx 0.3$ and 0.21 in Figs. 4b and 4c. Furthermore, besides the left end, the locations for the highest effect of the delamination are $\bar{L}_1\approx 0.6$ and 0.5, as shown in Figs. 4b and 4c. It can be seen from Table 3 that flutter is the only form of instability of the delaminated beam in all of the preceding cases. A different conclusion is derived from Fig. 4d in which the variation of the critical load is plotted at $\bar{k}=80$. The corresponding critical load for the healthy beam in this case is around $\bar{P}=2.32$. It can be observed from the figure that the delamination has the least effect when it is placed around $\bar{L}_1=0.45$, whereas it has the highest effect when is located around $\bar{L}_1=0.15$. The shape of the variation of the critical load is completely opposite to that observed in Figs. 4b and 4c in which flutter is the only instability form, as buckling is the only type of instability in the beam seen from Table 3.

The solution for the critical load $\bar{P}$ vs the location of delamination in longitudinal direction at $\bar{a}=0.1$ and 0.2 is listed in Table 4. It is observed that the critical load is independent of the location of the delamination for the shorter delamination and with the softer spring. On the other hand, for longer delamination the variation of the load vs the location of the delamination is similar to the solution obtained in Figs. 4a and 4c for flutter and buckling instability just discussed.

Conclusions

This paper presents a stability analysis of a delaminated beam, with the left end fixed and the right end restrained by a translational spring, subjected to a follower compressive force. Numerical simulations are conducted based on the mechanics model provided. The results show that the transition spring stiffness is almost the same with that of the healthy beam if shorter delamination is considered and the delamination is placed near the surface of the beam. Another observation is that the critical load decreases with increase in the location of the delamination in flexural direction. In addition, the buckling load decreases more obviously than the flutter load. The variation of the critical load vs the location in the longitudinal direction of the beam is investigated at different stiffnesses of the spring. The variation is not detectable for beams with shorter delamination. The results for longer delamination show that the delamination has the least effect on the stability of the beam at a location around a quarter of the beam from the left end if flutter occurs only on the beam, that is, the spring at the right end of the beam is with lower stiffness. This location moves toward the fixed end if the spring stiffness increases. Furthermore, the location of the delamination with the highest effect on the stability of the beam is around one-fourth the length from the right end of the beam. This location moves toward the fixed end as well if the spring stiffness increases. On the other hand, the shape of the variation of the buckling load, that is, when the spring stiffness is higher, is completely opposite to that observed in flutter analysis.

It is hoped that this research will provide a benchmark for the stability analysis of composite structures with delamination or other defects. Future studies will be focused on the stability analysis of delaminated beams with more general boundary conditions, such as free-free edges. Further investigation of nonlinear effect of the delamination on the flutter and/or buckling of delaminated beams should also be conducted.

Appendix: Nonzero Elements in Matrix [*C*] in Eq. (19)

$$N_1=\frac{L_2M_3-L_3M_2}{L_1M_2-L_2M_1},\qquad N_2=\frac{L_2M_4-L_4M_2}{L_1M_2-L_2M_1}$$

$$N_3=\frac{L_1M_3-L_3M_1}{L_2M_1-L_1M_2},\qquad N_4=\frac{L_1M_4-L_4M_1}{L_2M_1-L_1M_2}$$

$$L_1=-k_1^2\cos k_1L,\qquad L_2=-k_1^2\sin k_1L$$

$$L_3=k_2^2\cosh k_2L,\qquad L_4=k_2^2\sinh k_2L$$

$$M_1=k_1^3\sin k_1L-\frac{\bar{k}}{L^3}\cos k_1L$$

$$M_2=-k_1^3\cos k_1L-\frac{\bar{k}}{L^3}\sin k_1L$$

$$M_3=k_2^3\sinh k_2L-\frac{\bar{k}}{L^3}\cosh k_2L$$

$$M_4=k_2^3\cosh k_2L-\frac{\bar{k}}{L^3}\sinh k_2L$$

$$c_{11}=1,\qquad c_{13}=1,\qquad c_{19}=-(\cosh k_2L_1-\cos k_1L_1)$$

$$c_{1,10}=-\left(\sinh k_2L_1-\frac{k_2}{k_1}\sin k_1L_1\right)$$

$$c_{25}=1,\qquad c_{27}=1,\qquad c_{29}=-(\cosh k_2L_1-\cos k_1L_1)$$

$$c_{2,10}=-\left(\sinh k_2L_1-\frac{k_2}{k_1}\sin k_1L_1\right)$$

$$c_{32}=k_{11},\qquad c_{34}=k_{21},\qquad c_{39}=-(k_2\sinh k_2L_1+k_1\sin k_1L_1)$$

$$c_{3,10}=-(k_2\cosh k_2L_1-k_2\cos k_1L_1)$$

$$c_{46}=k_{12},\qquad c_{48}=k_{22},\qquad c_{49}=-(k_2\sinh k_2L_1+k_1\sin k_1L_1)$$

$$c_{4,10}=-(k_2\cosh k_2L_1-k_2\cos k_1L_1)$$

$$c_{51}=-\bar{t}^3k_{11}^2,\qquad c_{53}=\bar{t}^3k_{21}^2,\qquad c_{55}=-(1-\bar{t})^3k_{12}^2$$

$$c_{57}=(1-\bar{t})^3k_{22}^2$$

$$c_{59} = -\left(k_2^2 \cosh k_2 L_1 + k_1^2 \cos k_1 L_1\right) - \frac{\beta}{3a}(k_2 \sinh k_2 L_1 + k_1 \sin k_1 L_1)$$

$$c_{5,10} = -\left(k_2^2 \sinh k_2 L_1 + k_1 k_2 \sin k_1 L_1\right) - \frac{\beta}{3a}(k_2 \cosh k_2 L_1 - k_2 \cos k_1 L_1)$$

$$c_{5,11} = \frac{\beta k_1 N_3}{3a}, \qquad c_{5,12} = \frac{\beta}{3a}(k_2 + k_1 N_4)$$

$$c_{62} = -\bar{t}^3 k_{11}^3, \qquad c_{64} = \bar{t}^3 k_{21}^3, \qquad c_{66} = -(1-\bar{t})^3 k_{12}^3$$

$$c_{68} = (1-\bar{t})^3 k_{22}^3, \qquad c_{69} = -\left(k_2^3 \sinh k_2 L_1 - k_1^3 \sin k_1 L_1\right)$$

$$c_{6,10} = -\left(k_2^3 s \cosh k_2 L_1 + k_1^2 k_2 \cos k_1 L_1\right)$$

$$c_{71} = \cos k_{11} a, \qquad c_{72} = \sin k_{11} a, \qquad c_{73} = \cosh k_{21} a$$

$$c_{74} = \sinh k_{21} a, \qquad c_{7,11} = -(N_1 + 1), \qquad c_{7,11} = -N_2$$

$$c_{85} = \cos k_{12} a, \qquad c_{86} = \sin k_{12} a, \qquad c_{87} = \cosh k_{22} a$$

$$c_{88} = \sinh k_{22} a, \qquad c_{8,11} = -(N_1 + 1), \qquad c_{8,11} = -N_2$$

$$c_{91} = -k_{11} \sin k_{11} a, \qquad c_{92} = k_{11} \cos k_{11} a, \qquad c_{93} = k_{21} \sinh k_{21} a$$

$$c_{94} = k_{21} \cosh k_{21} a, \qquad c_{9,11} = -k_1 N_3, \qquad c_{9,12} = -(k_2 + k_1 N_4)$$

$$c_{10,5} = -k_{12} \sin k_{12} a, \qquad c_{10,6} = k_{12} \cos k_{12} a$$

$$c_{10,7} = k_{22} \sinh k_{22} a, \qquad c_{10,8} = k_{22} \cosh k_{22} a$$

$$c_{10,11} = -k_1 N_3, \qquad c_{10,12} = -(k_2 + k_1 N_4)$$

$$c_{11,1} = -\bar{t}^3 k_{11}^2 \cos k_{11} a, \qquad c_{11,2} = -\bar{t}^3 k_{11}^2 \sin k_{11} a$$

$$c_{11,3} = \bar{t}^3 k_{21}^2 \cosh k_{21} a, \qquad c_{11,4} = \bar{t}^3 k_{21}^2 \sinh k_{21} a$$

$$c_{11,5} = -(1-\bar{t})^3 k_{12}^2 \cos k_{12} a, \qquad c_{11,6} = -(1-\bar{t})^3 k_{12}^2 \sin k_{12} a$$

$$c_{11,7} = (1-\bar{t})^3 k_{22}^2 \cosh k_{22} a, \qquad c_{11,8} = (1-\bar{t})^3 k_{22}^2 \sinh k_{22} a$$

$$c_{11,9} = -\frac{\beta}{3a}(k_2 \sinh k_2 L_1 + k_1 \sin k_1 L_1)$$

$$c_{11,10} = -\frac{\beta}{3a}(k_2 \cosh k_2 L_1 - k_2 \cos k_1 L_1)$$

$$c_{11,11} = -\left(k_2^2 - k_1^2 N_1\right) + \frac{\beta k_1 N_3}{3a}$$

$$c_{11,12} = k_1^2 N_2 + \frac{\beta}{3a}(k_1 + k_2 N_4)$$

$$c_{12,1} = \bar{t}^3 k_{11}^3 \sin k_{11} a, \qquad c_{12,2} = -\bar{t}^3 k_{11}^3 \cos k_{11} a$$

$$c_{12,3} = \bar{t}^3 k_{21}^3 \sinh k_{21} a, \qquad c_{12,4} = \bar{t}^3 k_{21}^3 \cosh k_{21} a$$

$$c_{12,5} = (1-\bar{t})^3 k_{12}^3 \sin k_{12} a, \qquad c_{12,6} = -(1-\bar{t})^3 k_{12}^3 \cos k_{12} a$$

$$c_{12,7} = (1-\bar{t})^3 k_{22}^3 \sinh k_{22} a, \qquad c_{12,8} = (1-\bar{t})^3 k_{22}^3 \cosh k_{22} a$$

$$c_{12,11} = k_1^3 N_3, \qquad c_{12,12} = -\left(k_2^3 - k_1^3 N_4\right)$$

Acknowledgments

The authors are indebted to the reviewers for their invaluable comments on their final version of the research manuscript.

References

[1]Timoshenko, S. P., and Gere, J. M., *Theory of Elastic Stability*, McGraw–Hill, Singapore, 1961.

[2]Bolotin, V. V., *Non-Conservative Problems of the Theory of Elastic Stability*, Macmillan, New York, 1963.

[3]Feodos'ev, V. I., *Selected Problems and Questions in Strength of Materials*, Gostekhizdat, 1953.

[4]Pfluger, A., *Stabilitats Probleme der Elastostatik*, Springer-Verlag, Berlin, 1950.

[5]Beck, M., "Die Knicklast des Einseitig Eingespannten Tangential Gedruckten Stabes," *Zeitschrift für Angew. Math. Phys.*, Vol. 3, 1952.

[6]Carr, J., and Malhardeen, M. Z. M., "Beck's Problem," *SIAM Journal of Applied Mathematics*, Vol. 37, 1979, pp. 261, 262.

[7]Leipholz, H., "Assessing Stability of Elastic Systems by Considering Their Small Vibrations," *Ingenieur-Archiv*, Vol. 53, No. 5, 1983, pp. 345–362.

[8]Deineko, K. S., and Leonov, M. I., "The Dynamic Method of Investigating the Stability of a Bar in Compression," *PMM*, Vol. 19, 1955.

[9]Sundararajan, C., "Influence of an Elastic End Support on the Vibration and Stability of Beck's Column," *International Journal of Mechanical Science*, Vol. 18, No. 5, 1976, pp. 239–241.

[10]Kounadis, A., "Divergence and Flutter Instability of Elastically Restrained Structures Under Follower Forces," *International Journal of Engineering Science*, Vol. 19, No. 4, 1983, pp. 553–562.

[11]Kounadis, A. N., "The Existence of Regions of Divergence Instability for Nonconservative Systems Under Follower Forces," *International Journal of Solids and Structures*, Vol. 19, No. 8, 1983, pp. 725–733.

[12]Kounadis, A. N., "Some New Instability Aspects for Nonconservative Systems Under Follower Loads," *International Journal of Mechanical Science*, Vol. 33, No. 4, 1991, pp. 297–311.

[13]Bolotin, V. V., Grishko, A. A., Kounadis, A. N., and Gants, C. J., "Non-Linear Panel Flutter in Remote Post-Critical Domains," *International Journal of Non-Linear Mechanics*, Vol. 33, No. 5, 1998, pp. 753–764.

[14]Ryu, S.-U., and Sugiyama, Y., "Computational Dynamics Approach to the Effect of Damping on Stability of a Cantilevered Column Subjected to a Follower Force," *Computers and Structures*, Vol. 81, No. 4, 2003, pp. 265–271.

[15]Langthjem, M. A., and Sugiyama, Y., "Optimum Design of Cantilevered Columns Under the Combined Action of Conservative and Nonconservation Loads: Part I: The Undamped Case," *Computers and Structures*, Vol. 74, 2000, pp. 385–398.

[16]Anderson, S. B., and Thompsen, J. J., "Post-Critical Behaviour of Beck's Column with a Tip Mass," *International Journal of Non-Linear Mechanics*, Vol. 37, 2002, pp. 131–151.

[17]Wang, Q., "On Complex Flutter and Buckling Analysis of a Beam Structure Subjected to Static Follower Force," *Structural Engineering and Mechanics, An International Journal*, Vol. 16, No. 5, 2003, pp. 533–556.

[18]Wang, Q., and Lim, T. C., "Complex Analysis of Flutter and Buckling of Beams Under Rotational and Transverse Spring Constraints," *Advances in Structural Engineering*, Vol. 7, No. 1, 2004, pp. 21–31.

[19]Ohshima, T., and Sugiyama, Y., "Effect of Aerodynamic Loads on Dynamic Stability of Slender Launch Vehicle Subjected to an End Rocket Thrust," American Society of Mechanical Engineers, ASME International Mechanical Engineering Congress and Exposition, New Orleans, LA, Nov. 2002.

[20]Anyfantis, N., and Dimarogonas, A., "Stability of Columns with a Single Crack Subjected to Follower and Vertical Loads," *International Journal of Solids and Structures*, Vol. 19, No. 4, 1983, pp. 281–291.

[21]Dimarogonas, A. D., and Paipetis, S. A., *Rotor Dynamics*, Elsevier, London, 1983.

[22]Liebowitz, H., Vandervelt, H., and Harris, D. W., "Carrying Capacity of a Notched Column," *International Journal of Solids and Structures*, Vol. 3, 1967, pp. 489–500.

[23]Wang, Q., "Complete Stability Analysis of Cracked Beam Structures Subjected to Follower Compressive Load," *International Journal of Solids and Structures*, Vol. 41, No. 18, 2004, pp. 4875–4888.

[24]Wilkins, D. J., Elsermann, J. R., Camin, R. A., Margolis, W. S., and Benson, R. A., "Characterizing Delamination Growth in Graphite-Epoxy," *Damages in Composite Materials*, ASTE STP, 1982, pp. 168–183.

[25]Yin, W. L., Sallam, S. N., and Simitses, G. L., "Ultimate Axial Load Capacity of a Delaminated Beam-Plate," *AIAA Journal*, Vol. 24, No. 1, 1986, pp. 123–128.

[26]Simitses, G. J., Sallam, S. N., and Yin, W. L., "Effect of Delamination of Axially Loaded Homogeneous Laminated Plates," *AIAA Journal*, Vol. 23, No. 9, 1985, pp. 1437–1444.

[27]Bottega, W. J., and Maewall, A., "Delamination Buckling and Growth in Laminates," *Journal of Applied Mechanics*, Vol. 50, No. 4A, 1983, pp. 184–189.

[28]Troshin, V. P., "Effect of Longitudinal Delamination in a Laminar Cylindrical Shell on the Critical External Pressure," *Journal of Composite Materials*, Vol. 17, 1983, pp. 563–567.

[29]Peck, S. O., and Springer, G. S., "The Behavior of Delaminations in Composite Plates—Analytical and Experimental Results," *Journal of Composite Materials*, Vol. 25, No. 7, 1991, pp. 907–927.

[30]Lee, S., Park, T., and Voyiadjis, G. Z., "Free Vibration Analysis of Axially Compressed Laminated Composite Beam-Columns with Multiple Delaminations," *Composites Part B*, Vol. 33, No. 8, 2002, pp. 605–617.

[31]Luo, H., and Hanagud, S., "Delamination Detection Using Dynamic Characteristics of Composite Plates," *Proceedings of the 36th AIAA/ASME/ASCE/AHS Structures, Structural Dynamics, and Materials Conference*, Vol. 1, AIAA, Washington, DC, 1995, pp. 129–139.

[32]Lestari, W., and Hanagud, S., "Health Monitoring of Structures: Multiple Delamination Dynamics in Composite Beams," AIAA Paper 99-1509, 1999.

[33]Wang, Q., and Koh, C. G., "On the Region of Flutter and Buckling Instability for a Cracked Beam," *AIAA Journal*, Vol. 41, No. 11, 2003, pp. 2302–2304.

A. Berman
Associate Editor